UNDER REVIEW

RESCIENCE C

Replication / Machine Learning

[Re] When Does Label Smoothing Help?

Sven Dominik Wagner[1,†], Yann Philipp Kurowski[1,†], Leonhard Moritz Holländer[1,†], and Tobias Uelwer[1]
[1]TU Dortmund University, Department of Computer Science, Dortmund, Germany – [†]Equal contribution

Edited by
(Editor)

Received
01 November 2018

Published
–

DOI
–

Abstract Label smoothing is a technique that can make neural network classifiers less overconfident in their predictions and reduce overfitting, resulting in more reliable and accurate results. It's widely used but poorly understood. The replicated paper on label smoothing presents empirical evidence that it improves generalization and model calibration, and investigates its behavior in knowledge distillation. In this report, we seek to validate the authors' findings by re-implementing the original experiments, including the models and datasets, using PyTorch. Moreover, we evaluate the experiments on additional datasets and models, which align with the authors' conclusions. Furthermore, we reproduce the analysis of the penultimate layer representations and provide a detailed recipe for their calculation.

A replication of Rafael Müller, Simon Kornblith, and Geoffrey E. Hinton. When does label smoothing help? In Advances in Neural Information Processing Systems, pages 4696-4705, 2019.

1 Introduction

Neural networks are widely recognized as the predominant tool in machine learning due to their high adaptability. They can be utilized for various tasks, with classification emerging as one of the most prevalent ones. In classification tasks, the neural network receives various forms of data (e.g., images, audio data, tabular data) as its input and produces an estimate of the data's classification (e.g., what object is seen in an image) from a set of predefined labels.
When designing and training a neural network, the objective is twofold: accurate results for the training data and the ability to produce accurate results for new, unseen test data. However, neural networks tend to overfit, which can be arbitrarily complicated to avoid for complex models. Furthermore, modern neural networks are prone to provide predictions with high certainty even when those predictions are incorrect (or uncertain), making them overconfident. To address these issues, there are various techniques available, including the relatively new technique of label smoothing. This technique is designed to have a minimal impact on training time while protecting against both overfitting and overconfidence.

1.1 What Is Label Smoothing?

Label smoothing is a regularization method aiming to reduce overfitting and overconfidence in classification tasks. It was first introduced by Szegedy et al. [1]. The idea of label smoothing is to combine the one-hot encoded original label y with a discrete uniform distribution. The new label vector called y^{LS} has the components

$$y_k^{LS} = y_k(1-\alpha) + \alpha/K,$$

where K represents the number of distinct classes and $\alpha \in [0,1)$ is called *label smoothing constant* that determines the strength of the smoothing. The impact of label smoothing

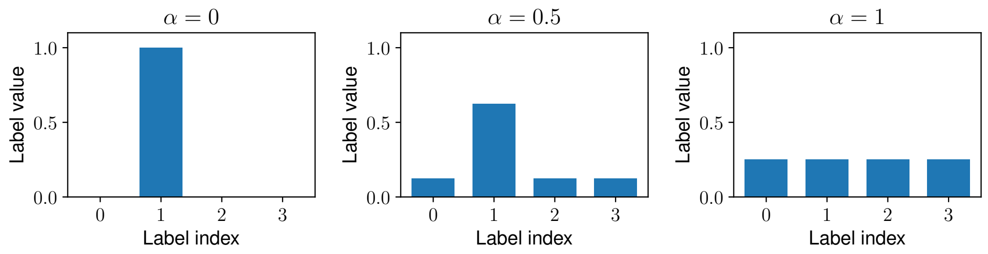

Figure 1. Visualization of different label smoothing constants on a hard label vector with class 1.

on a hard label vector is demonstrated in Figure 1. As α increases, the smooth label vector becomes more uniform. Compared to other methods, label smoothing has a negligible effect on training duration since it only modifies the label vector.

2 Overview Of Models and Datasets

A summary of our experiments is presented in Table 1, which outlines the different combinations of datasets and architectures that were utilized. A more detailed overview is given in the Appendix (see Table 5).

Table 1. Overview of all considered model and dataset combinations.

Architecture	Datasets
FCN	MNIST, EMNIST, FMNIST
AlexNet	CIFAR-10
ResNet-34	CUB-200-2011
ResNet-50	Tiny ImageNet
ResNet-56	CIFAR-10, CIFAR-100
Transformer	Multi30k

2.1 Datasets

In order to demonstrate the positive impact of label smoothing, the authors made use of five distinct networks and datasets. To validate their findings, we replicated the reported results as closely as possible. To further strengthen the points made by the authors, we also trained additional networks on a multitude of other datasets.

MNIST — The authors used the standard *MNIST* dataset [2] with 28×28 pixel images and ten different label classes. Here, the full $60,000$ training images were used for training, and the $10,000$ test images were used to show the results. For training, the images were randomly shifted by 2 pixels in the x and y directions, and no standardization was used.

Extended MNIST (EMNIST) — The *Extended MNIST* dataset [3] extends the standard MNIST dataset to also include lowercase and uppercase letters while keeping the structure of 28×28 pixel images. Whereas the original dataset includes all 62 classes, the subset we used includes only 47 balanced classes for a total of $112,800$ training and $18,800$ test images. In this balanced dataset, some lowercase letters were removed since they were too similar to their corresponding uppercase letter. In our experiments, we also kept the augmentation from the standard MNIST dataset.

FMNIST — The *FMNIST* dataset [4] reimagines the standard MNIST dataset to contain ten classes of fashion products while keeping the structure of 28×28 pixel images. Like the standard MNIST dataset, FMNIST also includes $60,000$ training and $10,000$ test images. In our experiments, we also kept the augmentation from the standard MNIST dataset.

CIFAR-10 — The authors used the standard CIFAR-10 dataset [5] with 32×32 pixel images and ten different label classes. While the original dataset consists of $50,000$ training images and $10,000$ test images, the authors only used $40,000$ images for training and the remaining $10,000$ training images to show results. All images were standardized per image. This means that the color values of each image were subtracted by their mean and divided by their standard deviation. Also, each image from the training dataset was augmented using random horizontal flips and random crops of the original 32×32 image to a 24×24 image. In our experiments, we kept most augmentation methods but used per-channel instead of per-image standardization. Furthermore, we used the full $50,000$ training images and the $10,000$ test images to show the results.

CIFAR-100 — The authors also used the standard CIFAR-100 dataset [5] with 32×32 pixel images and 100 different label classes. The same split, standardization, and augmentation as for CIFAR-10 were used. Instead of the random crops from 32×32 to 24×24 pixels, padded 40×40 pixel images were used with random crops to 32×32 pixels.

CUB-200-2011 — The Caltech-UCSD Birds-200-2011 Dataset [6] or more commonly known as CUB-200-2011 is an extended version of the CUB-200 dataset [7]. It contains a total of $11,788$ images, of which 5994 are used for training and 5794 for testing. There are a total of 200 classes, each representing a different bird species. Further, there are also annotations for each image, including part locations, binary attributes, and bounding boxes, which are not used in the classification. For the data augmentation, we employed random affine rotations with up to 45 degrees, random affine translations up to 0.35, and affine scaling between 0.65 and 1.35. As the images do not have a uniform size or aspect ratio in the dataset, we then resized them to 256×256 pixels. Lastly, there is a 50% chance that the image is flipped horizontally.

Tiny ImageNet — The authors used the well-known ImageNet/ILSVRC dataset with 224×224 images, which each belong to one of 1000 distinct classes. Due to the considerable size of approximately 1.2 million images and the training time required, this was out of the feasible range for our available resources. Instead, we made use of Tiny ImageNet, which uses 64×64 sized samples from ImageNet and 200 selected classes. The Tiny ImageNet dataset contains $100,000$ training images, $10,000$ validation images, and $10,000$ test images, which aligns better with our rather restricted resources. Tiny ImageNet was introduced as a classification challenge [8], and the original dataset can be found at the Stanford University website[1]. Analog to CUB-200-2011, we made use of affine rotations up to 7.5 degrees, affine translations up to 0.1, and affine scaling between 0.925 and 1.075. Each image then has a 50% chance to be flipped horizontally.

Multi30k — The authors used the WMT 2014 English to German dataset [9], which consists of around 4.5 million sentence pairs. Due to training time requirements and memory constraints, we had to fall back to the much smaller Multi30k dataset [10]. It contains images with descriptions in English and German. We only used the descriptions in training a Transformer model for language translation.

[1]http://cs231n.stanford.edu/tiny-imagenet-200.zip

2.2 Neural Network Models and Training

While the authors used TensorFlow [11] to implement the networks, we re-implemented these networks in PyTorch [12] to ensure both comparability and enhance accessibility. We used the original paper's structure, parameters, settings, and training methods whenever they were given and applicable.

Fully-connected Network (FCN) — The authors conducted their initial experiment on knowledge distillation using a standard neural network. This network had two hidden layers and utilized ReLU activation, as outlined in [13]. The network was used in two different variants, with 1200 and 800 neurons in each hidden layer, respectively. Although the authors did not provide specific values for dropout, we used 0.5 based on information found in [14].
For training the network, we first used a batch size of 512 because it massively boosts performance without impacting the accuracy of the network, even though the authors do not state the usage of batches. We trained for 100 epochs and linearly decreased the learning rates from 1 in the first layer and 0.1 in the second layer to 0. We also used stochastic gradient descent, which was not explicitly stated in the paper, with momentum and dampening of 0.9. These parameters correspond to the mentioned gradient smoothing. We used cross-entropy loss as a loss function.

AlexNet — The authors' implementation of AlexNet differs significantly from the original version [15]. In contrast to the five convolutional layers with up to 384 channels used in the original, the authors employ only two convolutional layers with a maximum of 64 channels. Additionally, the linear layers are also altered to accommodate the changes in the convolutional layers. This deviation is due to the fact that the model is solely intended for use with CIFAR-10 images that are 24×24 pixels in size. In contrast, the original AlexNet was created for ImageNet with images of size 224×224 pixels.
For training the network on CIFAR-10, we first used a batch size of 128 and trained for 1246 epochs or $389,998$ iterations. We used stochastic gradient descent without momentum and implemented a learning rate scheduler starting with a learning rate of 0.1 and dropping by a factor of 10 at epochs 415 and 830, respectively. Additionally, weight decay of $4 \cdot 10^{-2}$ was employed for the last two fully-connected layers, and the used cross-entropy loss was multiplied by a factor of 3, as suggested by the authors.

ResNet-34 — For the classification on the Cub-200-2011 dataset, the official implementation of ResNet-34 in PyTorch[2] was used with the pre-trained weights for ImageNet. The PyTorch implementation is based on the original ResNet paper [16].
For the training of Cub-200-2011, we used stochastic gradient descent with a learning rate of 0.3 and weight decay of 10^{-5} for a total of 250 epochs. Additionally, we applied a scheduler that multiplies the learning rate by 0.9 every 10 epochs. Each batch contained 256 images.

ResNet-50 — Analog to ResNet-34, the official implementation of ResNet-50 in PyTorch[2] was utilized with the pre-trained weights V2 for ImageNet. The PyTorch implementation is based on the original ResNet paper [16].
For the training of Tiny ImageNet, we utilized stochastic gradient descent with a learning rate of 0.004 with a weight decay of 10^{-5} and a momentum of 0.9 for a total of 100 epochs. Furthermore, we applied a scheduler that multiplies the learning rate by 0.5 every 7 epochs.

[2]https://pytorch.org/vision/main/models/resnet.html

ResNet-56 — For the ResNet-56 architecture, the authors use a modified official TensorFlow implementation. This version is based on the ResNet implementation for CIFAR-10 from the original ResNet paper [16] but with preactivation added (as described in [17]). For CIFAR-100, the implementation also uses a convolution with filter size 7×7, while the standard filter size of 3×3 is used for CIFAR-10.
For both training on CIFAR-10 and CIFAR-100, we used the same methods. As stated in the paper, we used batches of 128 and trained for 205 epochs or $64,165$ iterations. We used stochastic gradient descent for training, incorporating a Nesterov momentum of 0.9. Additionally, we implemented a learning rate scheduler starting with a rate of 0.1 and decreasing by a factor of 10 at epochs 102 and 153. We also used weight decay of 10^{-4} and multiplied the used cross-entropy term by a factor of 3, as recommended in the paper. Finally, we utilized gradient clipping with a maximum threshold of 1.

Transformer — The Transformer is an encoder-decoder network architecture introduced in 2017 by Vaswani et al. [18]. It is based upon the so-called attention mechanism. The attention mechanism is responsible for capturing relationships between words in a sequence. It allows the model to assign values to each word pair while processing the input. This value represents the relationship between the two words. Thanks to this, transformers can efficiently process long-range dependencies and achieve state-of-the-art performance in various natural language processing tasks. The authors use the original Transformer architecture [18] with the same hyperparameters for exploring the effects of label smoothing on a language translation task. We use the sequence-to-sequence model implemented by PyTorch in their example for language translation using transformer [19]. It is a down-scaled version of the original transformer network. This model has three encoder and decoder layers instead of six, while also using 512 instead of 2048 dimensions for the inner feed-forward networks.

3 Accuracy with Label Smoothing

In the original work, the authors claimed that label smoothing has a positive impact on the test accuracy of a trained network. For this, multiple examples were provided, where networks were trained with varying values of the label smoothing constant α.

Table 2. Top-1 classification accuracies of networks trained with and without label smoothing compared with the results from Müller et al. [20]. Best results are printed **bold**.

		Accuracy [%]				
Dataset	Architecture	$\alpha = 0.0$	$\alpha = 0.05$	$\alpha = 0.1$	$\alpha = 0.15$	$\alpha = 0.30$
MNIST	FCN (ours)	99.06	**99.33**	99.31	99.24	99.13
EMNIST	FCN (ours)	88.79	89.11	**89.35**	89.19	88.88
FMNIST	FCN (ours)	**91.01**	90.66	90.45	90.59	90.37
CIFAR-10	AlexNet [20]	**86.8**	-	86.7	-	-
	AlexNet (ours)	85.01	85.13	85.47	84.83	**86.02**
	ResNet-56 (ours)	93.59	**93.62**	93.33	93.55	93.53
CIFAR-100	ResNet-56 [20]	72.1	-	**72.7**	-	-
	ResNet-56 (ours)	71.61	71.99	**72.07**	71.74	71.75
CUB-200-2011	ResNet-34 (ours)	77.75	80.38	80.48	**81.12**	80.77
TinyImageNet	ResNet-50 (ours)	72.20	72.65	72.30	72.28	**72.75**
ImageNet	Inception-v4 [20]	**80.9**	-	**80.9**	-	-

As shown in Table 2 we were able to verify these results and observed the same trend for additional architectures and datasets. Our extensive evaluation shows that implementing moderate levels of label smoothing can effectively reduce overfitting and increase the accuracy of the networks overall. The level of label smoothing required to effectively mitigate overfitting and improve accuracy varies between architectures and datasets. While some models benefit significantly from high label smoothing constants (e.g., AlexNet on CIFAR-10), others only exhibit minor improvements or even degradation from small constants (e.g., ResNet-56 on CIFAR-10 / FCN on FMNIST).

4 Penultimate Layer Representation

The authors propose a visualization scheme that illustrates how label smoothing affects the activations of the penultimate layer and the output of the network. For a single data point, neural network classifiers calculate a prediction

$$p_k = \frac{\exp\left(a^T w_k\right)}{\sum_{l=1}^{K} \exp\left(a^T w_l\right)} \tag{1}$$

for the k-th class by applying the softmax to the logit $a^T w_k$, where $a \in \mathbb{R}^n$ is the activation vector of the penultimate layer and w_k is the weight vector for the k-th class of the last layer. The weight vector $w_k \in \mathbb{R}^n$ can be seen as a template of class k. The authors state, that the logits depend on the Euclidean distance $||a - w_k||^2$ between the activations of the penultimate layer a and the template w_k. To visualize a high-dimensional activation a in two dimensions, we first choose three classes and their corresponding templates w_1, w_2, and w_3. To find the plane passing through the templates, we subtract the third template from the first and second template, resulting in vectors $\Delta_1 = w_1 - w_3$ and $\Delta_2 = w_2 - w_3$. After that, we define the matrix

$$A = \begin{bmatrix}\Delta_1 \ \Delta_2\end{bmatrix} \in \mathbb{R}^{n \times 2},$$

which contains the vectors Δ_1 and Δ_2 as columns. Next, we orthogonalize A by calculating its QR decomposition $A = QR$, where $Q \in \mathbb{R}^{n \times 2}$ is an orthogonal matrix and $R \in \mathbb{R}^{2 \times 2}$ is an upper triangular matrix. After normalizing the column vectors of Q, we obtain two vectors $u \in \mathbb{R}^n$ and $v \in \mathbb{R}^n$, which are orthogonal vectors that form the basis of a two-dimensional vector subspace. We can project the activation now into the subspace. The subspace coordinates are given by $\lambda = a^T u$ and $\mu = a^T v$.
For the visualization, we choose a number of data points from the three picked classes and produce a scatter plot of their subspace coordinates. A possible implementation can be found in Section A.1. According to Müller et al. [20], label smoothing promotes the tendency for the activations of the second-to-last layer to align closely with the reference pattern of the accurate class, while maintaining an equitable separation from the reference patterns of the inaccurate classes.

Results – We were able to reproduce the effect described in the paper as seen in Figure 2. For CIFAR-10, we chose the classes airplane (red), automobile (green), and bird (blue). For CIFAR-100, we chose apple (red), aquarium_fish (green), and baby (blue). For MNIST, we chose zero (red), one (green), and two (blue). The effect on the clusters is clearly visible, as when training with label smoothing, the clusters become much denser and equidistant (i.e., the shape is more triangular). Also, the distance between the templates is much smaller, which can be seen by looking at the scale of the axes.

5 Implicit Model Calibration

The authors compared the model calibration of multiple models trained with hard labels and smooth labels to demonstrate the improvement of results with smooth labels.

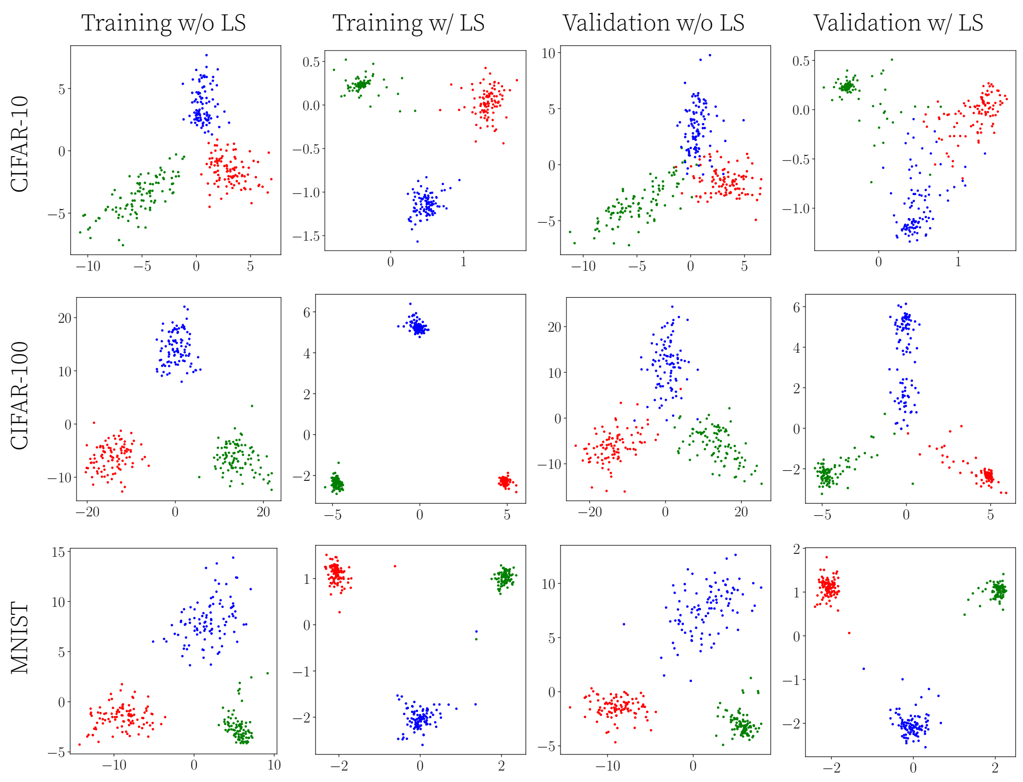

Figure 2. Visualization of the penultimate layer activations: AlexNet on CIFAR-10 (first row), ResNet-56 on CIFAR-100 (second row), FCN on MNIST (third row).

Additionally, they applied temperature scaling to the models trained with hard labels to improve their calibration. The evaluation was performed using the *expected calibration error (ECE),* followed by the corresponding reliability diagrams.

In the original paper, the model calibration was examined on ResNet-56, InceptionV4, and the Transformer architecture. While ResNet-56 and InceptionV4 were used for classification on the CIFAR-100 and ImageNet datasets, the Transformer was trained on the Multi30k dataset to translate text from English to German.
One of the primary objectives of label smoothing is to improve the calibration of neural networks. The calibration can be described as the difference between accuracy and confidence. A poorly calibrated network exhibits a high difference, while a well-calibrated network shows a low difference. While the accuracy of a network is a common measure, confidence is primarily evaluated in the context of model calibration. The confidence for a given input example x is given by the highest output provided by the network on that input through

$$\mathrm{conf}(x) = \max_k \{p_k(x)\},$$

where p_k is the k-th output of the neural network.
A technique that is frequently used to calibrate a trained network is *temperature scaling* [21]. Temperature scaling applies a temperature $\tau > 0$ to the logits before applying the softmax normalization as described by

$$p_k^\tau = \frac{\exp(z_k/\tau)}{\sum_{i=1}^{K} \exp(z_i/\tau)},$$

where p_k refers to the k-th prediction and z_k refers to the k-th logit of the network. Thus each logit is divided by the temperature before the softmax normalization is applied.

This technique is used to explicitly calibrate a network, as it only affects the confidence without impacting the accuracy. Using a high temperature ($\tau > 1$) decreases the confidence while employing a low temperature ($\tau < 1$) would increase the confidence. When $\tau = 1$ is used, temperature scaling has no effect, as it effectively becomes a division by 1.

A common index to measure the calibration of a network is the *expected calibration error (ECE)* [22]. This index estimates the calibration of a network based on a set of test examples. To calculate the ECE, the output of the network is calculated over every example, and these are then separated into B distinct bins according to their confidence. For example, the bin b would include all examples x, where $\text{conf}(x) \in \left[\frac{b}{B}, \frac{b+1}{B}\right)$. Over each of those bins, the ECE can be calculated like

$$ECE = \sum_{b=1}^{B} \frac{n_b}{N} |\,\text{conf}(b) - \text{acc}(b)|,$$

where n_b is the number of examples in bin b, N is the total amount of samples, $\text{conf}(b)$ is the average confidence over all examples in b and $\text{acc}(b)$ is the accuracy over all examples in b. In general, a lower ECE is preferred and indicates a better calibrated network.

One way to visualize the calibration is a confidence-accuracy plot or *reliability diagram*. For the diagram, the bins are calculated as above, along with their confidence and accuracy. Each bin then correlates to a point in a confidence-accuracy plot, providing a more detailed description of the network calibration. In the optimal case, each of the bin's accuracy and confidence values would be equal, resulting in a straight line. In such a case, the network would be perfectly calibrated, as the confidence and accuracy always align. For the following plots and ECE computations, the number of bins is consistently set to 15 to align with the original paper.

5.1 Model Calibration for Classification

In this experiment, we compared the ECE for several network architectures on different datasets. To further examine the impact of different degrees of label smoothing on the calibration, we used several different label smoothing constants for each network. Following the methodology of the original paper, the models trained on hard labels were also improved by temperature scaling and compared with the other models. While the experiment in the original paper only evaluated three different architectures, we took a more quantitative approach and evaluated several additional combinations of different architectures and datasets. This evaluation thus allows a much broader understanding of the effects of label smoothing on network calibration.
The results of this evaluation are presented in Table 3. Here one can see that using small label smoothing constants in training can help to implicitly calibrate a neural network. In most experiments, the ECE became smaller when using label smoothing. Although temperature scaling still remains the best technique when looking at the results, finding a fitting temperature for a network can often be tedious, as it includes evaluating the ECE for every reasonable temperature. But label smoothing does not seem to help in every case. For the fully-connected networks, even small label smoothing constants did not help. This is the case because these networks were not overconfident in their predictions but rather well-calibrated. For these scenarios, label smoothing is not the best method as it makes the network underconfident. This phenomenon can be observed in Figure 3a and 3b.
While the ResNet-56 trained with hard labels is rather overconfident (all points lie under the black line), both lines for the network trained with label smoothing and for the temperature-scaled network are very close to the black line and, as such, well-calibrated. For the fully-connected network, both the network trained with hard labels and the

Table 3. ECE for neural networks trained with and without label smoothing compared with temperature-scaled networks and the results from Müller et al. [20]. Best results are printed **bold**.

				ECE				
		$\alpha = 0.0$		$\alpha = 0.0$	$\alpha = 0.05$	$\alpha = 0.1$	$\alpha = 0.15$	$\alpha = 0.3$
DATASET	ARCHITECTURE	ECE	T	T = 1.0	T = 1.0	T = 1.0	T = 1.0	T = 1.0
MNIST	FCN (OURS)	0.001	1.06	**0.002**	0.056	0.102	0.147	0.281
EMNIST	FCN (OURS)	0.008	1.14	**0.017**	0.056	0.108	0.154	0.288
FMNIST	FCN (OURS)	0.008	1.1	**0.010**	0.042	0.085	0.128	0.252
CIFAR-10	ALEXNET (OURS)	0.012	2.5	0.097	**0.026**	0.048	0.087	0.221
	RESNET-56 (OURS)	0.006	3.1	0.049	**0.028**	0.065	0.102	0.222
CIFAR-100	RESNET-56 (OURS)	0.029	2.9	0.207	0.053	**0.043**	0.045	0.120
	RESNET-56 [20]	0.021	1.9	0.150	**0.024**	-	-	-
CUB-200-2011	RESNET-34 (OURS)	0.013	1.4	**0.082**	0.159	0.235	0.286	0.400
TinyImageNet	RESNET-50 (OURS)	0.013	1.7	0.150	0.060	**0.045**	0.054	0.166
ImageNet	INCEPTIONV4 [20]	0.022	1.4	0.071	-	**0.035**	-	-
Multi30k	TRANSFORMER (OURS)	0.058	1.8	0.449	0.475	0.372	0.222	**0.110**

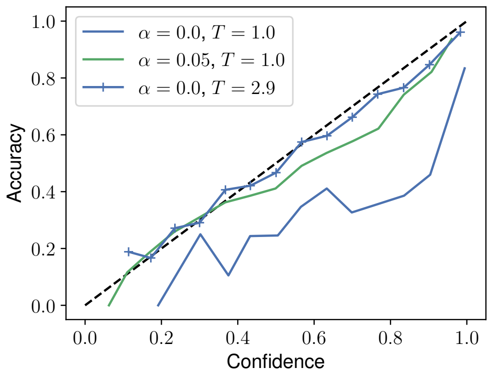

(a) ResNet-56 on the CIFAR-100 dataset

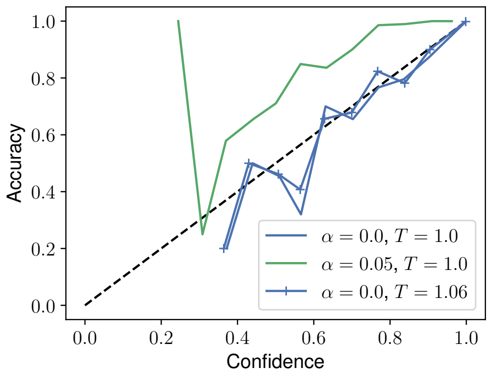

(b) Fully-connected network on the MNIST dataset

Figure 3. Reliability diagrams for classification networks. For ResNet-56, label smoothing resulted in a good calibration, while it caused underconfidence for the fully-connected network.

temperature-scaled network are rather well-calibrated, but the line for the network trained with label smoothing lies over the black line and, as such, is relatively underconfident.

5.2 Model Calibration on Transformer

When using a Transformer, we were also able to reproduce the trend of achieving a better calibration with label smoothing. When conducting the above experiment on the Transformer, we achieve a substantially better ECE score when label smoothing of $\alpha = 0.3$ is applied, which can be seen in Table 3. The same trend can be found in the corresponding reliability diagram (see Figure 4). But despite the improvements label smoothing provides, it is visible that the positive impact of temperature scaling is still stronger.

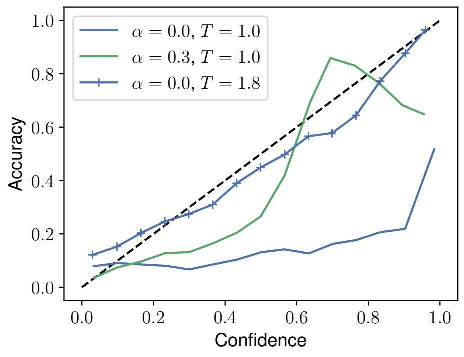

Figure 4. Reliability diagram for Transformer on the Multi30k dataset. Label smoothing caused a significantly better calibration.

5.3 Translation Quality on Transformer

The quality of language translations is commonly evaluated using the *bilingual evaluation understudy (BLEU) score* [23], which is based on the concept of n-grams. n-grams are sequences of n consecutive words in a sentence. To compare a generated sentence (also called ”candidate”) with a reference sentence, the percentage of n-grams from the candidate appearing in the reference is calculated. The result is known as the n-gram precision. This n-gram precision is calculated for all n-grams starting with $n = 1$ and ending with a specified maximum, which is typically $n = 4$. The BLEU score is then calculated as a weighted average of the different n-gram precision, while also incorporating a brevity penalty. This penalty helps to avoid overly short translations.

The *negative log-likelihood (NLL)* is commonly used as a loss function in multi-class classification. It has to be applied after the *softmax* activation function and is defined as

$$l(p, y) = -\log(p_n),$$

where p_n denotes the prediction of the network for the correct class. The NLL is up to a constant factor equivalent to the cross-entropy loss if no label smoothing is used. If label smoothing is used, it is not equivalent because NLL does not consider the predictions and labels for the incorrect classes.

The influence of temperature scaling and label smoothing on the ECE and the BLEU score are shown in Figure 5. Here it can be seen that the amount of temperature scaling needed to get a minimal ECE is decreased to about 1.1 when a label smoothing constant of $\alpha = 0.3$ is used. This corresponds to the results in the paper. We were not able to reproduce an increase in BLEU score by using label smoothing. In the rightmost panel, the effect on the NLL is plotted. The difference between smooth labels (orange) and hard labels (blue) is not large, but the smooth labels perform slightly better for low temperature values, while this trend reversed for higher ones. This differs from the results from the paper, where the hard labels had a better NLL for all temperatures.

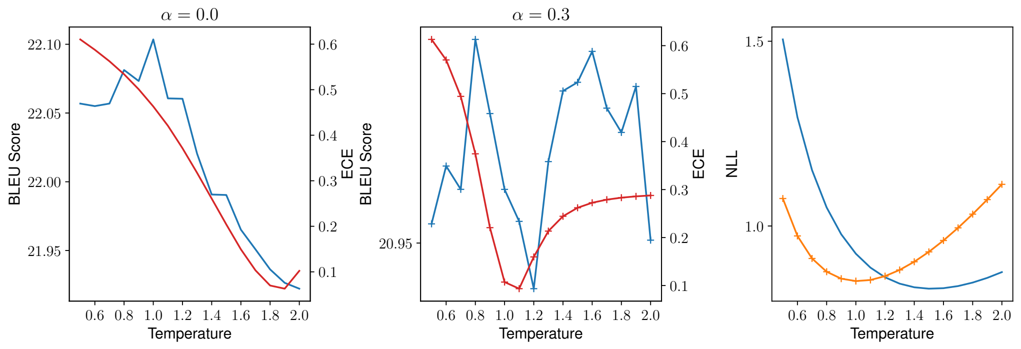

Figure 5. The effects of calibration on ECE, BLEU, and NLL for Transformer on the Multi30k dataset. In the first two panels, the blue line reflects the BLEU score, and the red line represents the ECE. Curves with markers correspond to networks trained with label smoothing.

6 Knowledge Distillation

The concept of knowledge distillation [13] is a common technique to train a small neural network (student) from the outputs of a large neural network (teacher). In this way, it is possible to achieve a higher accuracy of the student network compared to usual supervised training. The rationale is that the knowledge that was extracted by the teacher network can help the training of the student network. A usual knowledge distillation procedure works as follows: first, a teacher network is trained as usual. After that, the student network is trained by minimizing the convex combination of two losses

$$L(y, p^\tau, q^\tau) = (1-\beta)H(y, q^\tau) + \beta H(p^\tau, q^\tau), \tag{2}$$

where H denotes the cross-entropy, $\beta \in [0, 1]$ is a hyperparameter that balances the two losses, and p^τ and q^τ are the scaled output probabilities of the teacher network and the student network after temperature scaling with temperature τ has been applied (refer to Section 5). The first term $H(y, q^\tau)$ is the usual cross-entropy between the ground-truth label and the output probabilities of the student network. The second term $H(p^\tau, q^\tau)$ is the cross-entropy between the output probabilities of the student network and the output probabilities of the teacher network. Figure 6 shows the abstract concept of

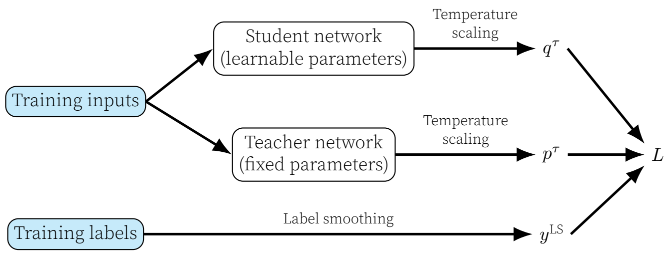

Figure 6. Knowledge distillation with label smoothing and temperature scaling.

knowledge distillation. Note that the temperature scaling is optional and can be omitted. In the following experiments, the temperature scaling for the student network was not included during its training process, as it is only a scalar that can be learned.
The authors also define a smoothness index

$$\gamma = \mathbb{E}\left[\sum_{k=1}^{K}(1-y_k)p_k^\tau K/(K-1)\right], \tag{3}$$

where y_k is the k-th entry of the label-vector, p_k^τ is the k-th component of the teacher output, and K is the number of output classes. This smoothness index allows us to compare models that use different combinations of label smoothing and temperature scaling and is computed over all training examples.

6.1 Distillation with Fully-connected Networks

In the first experiment, we trained a fully-connected teacher network with 1200 neurons per layer using dropout on MNIST. This teacher network was then used for the knowledge distillation of a fully-connected student network with 800 neurons per layer. The student network was trained on the non-augmented MNIST dataset without the use of dropout.
Instead of the loss function described in Equation (2), half the mean squared error for the second cross-entropy loss and $\beta = 0.6$ were used.
The same teacher was then trained without dropout, instead using label smoothing with $\alpha = 0.1$. The student network was distilled as before, without the use of dropout or augmentation of the dataset. While the teacher achieved a higher accuracy with label smoothing, the performance of the student network was significantly worse compared to before.

Table 4. Errors of the FCN networks trained on MNIST compared to the errors from Müller et al. [20].

Network	Müller et al.	Ours
Teacher w/o LS	0.67%	0.81%
Teacher w/ LS	0.59%	0.69%
Student w/o LS	0.74%	0.93%
Student w/ LS	0.91%	1.05%

As seen in Table 4, our errors were slightly higher than the reported results by the authors but still support this conclusion.

The authors also conducted the following experiment, originally on convolutional networks, which we extended to the fully-connected networks.
To establish a baseline, the authors first trained teacher networks $(M1)$ and student networks without distillation $(M2)$ using different label smoothing constants. Next, they trained student networks using distillation from a teacher with different temperature-scaled outputs but without label smoothing $(M3)$. Finally, they trained student networks using distillation from teachers with different label smoothing constants to demonstrate that a label-smoothed teacher does not distill well $(M4)$. When training $(M3)$ and $(M4)$, we use the aforementioned loss-function. The label smoothing constants used were $[0, 0.15, 0.3, 0.45, 0.6, 0.75]$ and the temperatures were $[1, 2, 4, 8, 12, 16]$.

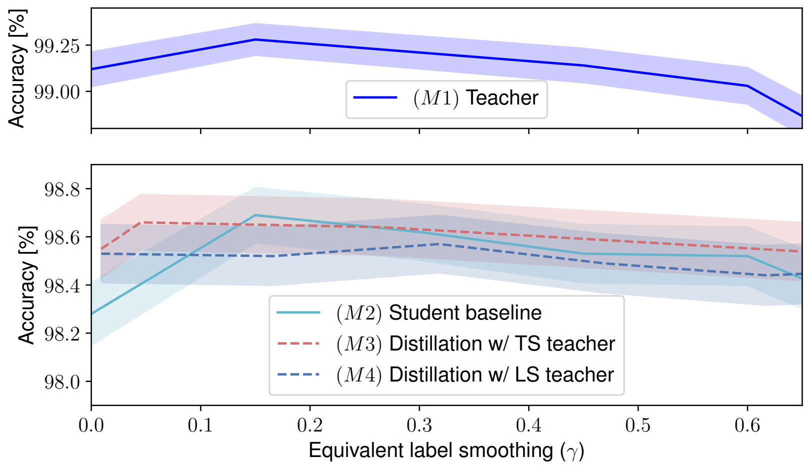

Figure 7. Performance of distillation from fully-connected architecture (1200 neurons) to fully-connected architecture (800 neurons) on MNIST. Shaded areas show the standard error.

The results of this experiment are displayed in Figure 7. For $(M1)$ and $(M2)$, γ is equivalent to α, while Definition (3) was applied to $(M3)$ and $(M4)$. Here one can see that the accuracy of the student baseline $(M2)$ is generally lower than the accuracy of the distillation with a temperature-scaled teacher $(M3)$. Furthermore, the conclusion that the student's accuracy decreases when the teacher is trained with label smoothing remains true when comparing $(M3)$ and $(M4)$.

6.2 Distillation with Convolutional Networks

The authors also conducted the above-mentioned experiment on convolutional networks, using ResNet-56 networks as teachers and AlexNet networks as students. The dataset used was CIFAR-10.
Our evaluation results for the models are presented in Figure 8. Although the overall results remain consistent, we noticed some discrepancies. While our teachers perform better overall than those in the paper, the accuracy does not improve when using label smoothing. In contrast, the student baseline showed a slight improvement when using label smoothing, which differs from the paper. As expected, the use of knowledge distillation with a temperature-scaled teacher enhanced the student's overall accuracy. Furthermore, the accuracy was negatively impacted when the student network was trained via distillation from a teacher using label smoothing. These results confirm the authors' statements and align with the described behavior in the paper.

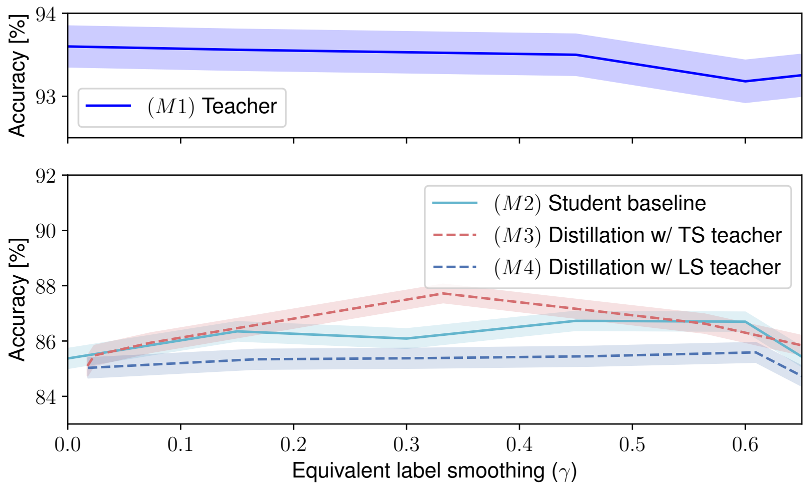

Figure 8. Performance of distillation from ResNet-56 to AlexNet on CIFAR-10. Shaded areas show the standard error.

6.3 Mutual Information

To further investigate the reasons for the worse performance when applying label smoothing to a teacher network, the authors compared the amount of information that is erased during the training with label smoothing. This is done by calculating the *mutual information* between the inputs and logits of the network which uses data augmentation as a source of randomness. Unfortunately, we were unable to reproduce the results from the original work using the described formula. We contacted the authors for clarification but we did not receive an answer.

7 Conclusion

In this report, we aimed to reproduce the results of the paper [20], which analyzed the impact of label smoothing on classification tasks, while we also provided a deeper insight into label smoothing. We successfully re-implemented the majority of the experiments from the paper in PyTorch and provided a concrete mathematical description of the penultimate layer visualization which was omitted in the original work. In detail, by comparing models trained with and without label smoothing, we were able to show that using smooth labels improves the accuracy of the models in most cases. Furthermore, we demonstrated that the penultimate layer representation of models trained with label smoothing exhibits more compact and better-structured clusters. We also confirmed the positive impact of label smoothing on model calibration for most classification cases. However, models that were already well-calibrated showed minimal to no improvements when trained on smooth labels. Due to resource constraints, validating the results for ImageNet on InceptionV4 was not feasible. We applied label smoothing to the training of our transformer model on a smaller dataset than the one used by the original authors. This resulted in an improvement of the model calibration and did not improve the translation quality. Furthermore, our findings confirm that using label smoothing in knowledge distillation has a negative impact on the accuracy of the student network. To support this claim, we expanded the experiment using additional models and datasets. In conclusion, we were able to reproduce a majority of the findings of Müller et al. [20] and validate the described behavior of label smoothing. In the cases of mutual information and experiments on the Transformer, we were not able to reproduce the results.

References

1. C. Szegedy, V. Vanhoucke, S. Ioffe, J. Shlens, and Z. Wojna. "Rethinking the Inception Architecture for Computer Vision." In: **Proceedings of the IEEE Conference on Computer Vision and Pattern Recognition**. IEEE Computer Society, 2016, pp. 2818–2826. arXiv:1512.00567.
2. Y. Lecun, L. Bottou, Y. Bengio, and P. Haffner. "Gradient-based learning applied to document recognition." In: **Proceedings of the IEEE** 86.11 (1998), pp. 2278–2324. DOI: 10.1109/5.726791.
3. G. Cohen, S. Afshar, J. Tapson, and A. van Schaik. "EMNIST: an extension of MNIST to handwritten letters." In: **Proceedings of the International Joint Conference on Neural Networks**. 2017, pp. 2921–2926. arXiv:1702.05373.
4. H. Xiao, K. Rasul, and R. Vollgraf. "Fashion-MNIST: a Novel Image Dataset for Benchmarking Machine Learning Algorithms." In: **CoRR** abs/1708.07747 (2017). arXiv:1708.07747.
5. A. Krizhevsky. "Learning multiple layers of features from tiny images." MA thesis. University of Toronto, 2009.
6. C. Wah, S. Branson, P. Welinder, P. Perona, and S. Belongie. **Caltech-UCSD Birds-200-2011**. Tech. rep. CNS-TR-2011-001. California Institute of Technology, 2011. URL: https://resolver.caltech.edu/CaltechAUTHORS:20111026-120541847.
7. P. Welinder, S. Branson, T. Mita, C. Wah, F. Schroff, S. Belongie, and P. Perona. "Caltech-UCSD Birds 200." In: (2010).
8. mnmoustafa. **Tiny ImageNet**. 2017. URL: https://kaggle.com/competitions/tiny-imagenet (visited on 08/01/2023).
9. O. Bojar et al. "Findings of the 2014 Workshop on Statistical Machine Translation." In: **Proceedings of the Ninth Workshop on Statistical Machine Translation**. Association for Computational Linguistics, 2014, pp. 12–58. DOI: 10.3115/v1/W14-3302.
10. D. Elliott, S. Frank, K. Sima'an, and L. Specia. "Multi30K: Multilingual English-German Image Descriptions." In: **Proceedings of the Workshop on Vision and Language**. The Association for Computer Linguistics, 2016. arXiv:1605.00459.
11. M. Abadi et al. "TensorFlow: Large-Scale Machine Learning on Heterogeneous Distributed Systems." In: **CoRR** abs/1603.04467 (2016). arXiv:1603.04467.
12. A. Paszke et al. "PyTorch: An Imperative Style, High-Performance Deep Learning Library." In: **Advances in Neural Information Processing Systems**. Curran Associates, Inc., 2019, pp. 8024–8035. arXiv:1912.01703.
13. G. E. Hinton, O. Vinyals, and J. Dean. "Distilling the Knowledge in a Neural Network." In: **CoRR** abs/1503.02531 (2015). arXiv:1503.02531.
14. G. E. Hinton, N. Srivastava, A. Krizhevsky, I. Sutskever, and R. Salakhutdinov. "Improving neural networks by preventing co-adaptation of feature detectors." In: **CoRR** abs/1207.0580 (2012). arXiv:1207.0580.
15. A. Krizhevsky, I. Sutskever, and G. E. Hinton. "ImageNet Classification with Deep Convolutional Neural Networks." In: **Advances in Neural Information Processing Systems**. 2012, pp. 1106–1114.
16. K. He, X. Zhang, S. Ren, and J. Sun. "Deep Residual Learning for Image Recognition." In: **Proceedings of the IEEE Conference on Computer Vision and Pattern Recognition**. IEEE Computer Society, 2016, pp. 770–778. arXiv:1512.03385.
17. K. He, X. Zhang, S. Ren, and J. Sun. "Identity Mappings in Deep Residual Networks." In: **Proceedings of the European Conference on Computer Vision**. Vol. 9908. Lecture Notes in Computer Science. Springer, 2016, pp. 630–645. arXiv:1603.05027.
18. A. Vaswani, N. Shazeer, N. Parmar, J. Uszkoreit, L. Jones, A. N. Gomez, L. Kaiser, and I. Polosukhin. "Attention is All you Need." In: **Advances in Neural Information Processing Systems**. 2017, pp. 5998–6008. arXiv:1706.03762.
19. PyTorch. **Language Translation with nn.Transformer and torchtext**. URL: https://pytorch.org/tutorials/beginner/translation_transformer (visited on 08/01/2023).
20. R. Müller, S. Kornblith, and G. E. Hinton. "When does label smoothing help?" In: **Advances in Neural Information Processing Systems**. 2019, pp. 4696–4705. arXiv:1906.02629.
21. C. Guo, G. Pleiss, Y. Sun, and K. Q. Weinberger. "On Calibration of Modern Neural Networks." In: **Proceedings of the International Conference on Machine Learning**. PMLR, 2017, pp. 1321–1330. arXiv:1706.04599.
22. M. P. Naeini, G. F. Cooper, and M. Hauskrecht. "Obtaining Well Calibrated Probabilities Using Bayesian Binning." In: **Proceedings of the AAAI Conference on Artificial Intelligence**. AAAI Press, 2015, pp. 2901–2907. DOI: 10.1609/aaai.v29i1.9602.
23. K. Papineni, S. Roukos, T. Ward, and W. Zhu. "Bleu: a Method for Automatic Evaluation of Machine Translation." In: **Proceedings of the Annual Meeting of the Association for Computational Linguistics**. ACL, 2002, pp. 311–318. DOI: 10.3115/1073083.1073135.

A Appendix

A.1 Code for Penultimate Layer Representation

Algorithm 1 Code for calculating the penultimate layer representation

```python
import numpy as np

# normalize a vector
def normalize(v):
    norm = np.linalg.norm(v)
    return v / norm


def qr_decomposition(points):
    # construct the matrix A from the templates
    A = np.zeros((2, points.shape[1]))
    A[0] = normalize(points[1] - points[0])
    A[1] = normalize(points[2] - points[0])

    # apply the QR decomposition
    Q, R = np.linalg.qr(A.T)

    # return the orthogonal matrix (orthonormal basis)
    return Q


# get w_1, w_2, and w_3
templates = penultimate_weights[class_indices]
# construct the matrix and apply the QR decomposition
orthonormal_basis = qr_decomposition(templates)

# project the penultimate layer activations on the plane for each class
for i in range(3):
    projection[i] = np.dot(penultimate_activations[i], orthonormal_basis)
```

A.2 Overview Over Experiments

Table 5. Overview of all model and dataset combinations and the experiments where these combinations were used. The used abbreviations are: Accuracy (Accuracy with label smoothing, see Section 3), PLR (Penultimate layer representation, see Section 4), IMC (Implicit model calibration, see Section 5), and KD (Knowledge distillation, see Section 6)

		EXPERIMENT			
DATASET	ARCHITECTURE	Accuracy	PLR	IMC	KD
MNIST	FC	✓	✓	✓	✓
EMNIST	FC	✓		✓	
FMNIST	FC	✓		✓	
CIFAR-10	ALEXNET	✓	✓	✓	✓
CIFAR-10	RESNET56	✓		✓	✓
CIFAR-100	RESNET-56	✓	✓	✓	
CUB-200-2011	RESNET-34	✓	✓	✓	
TINY IMAGENET	RESNET-50	✓	✓	✓	
MULTI30K	TRANSFORMER			✓	

A.3 Further Reliability Diagrams

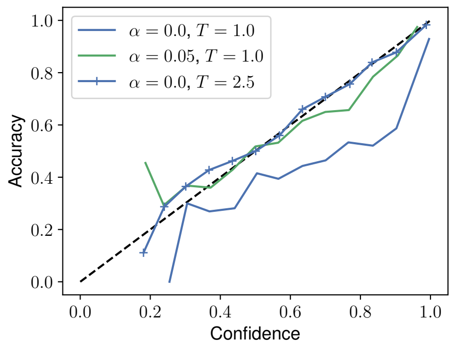

(a) AlexNet on the CIFAR-10 dataset

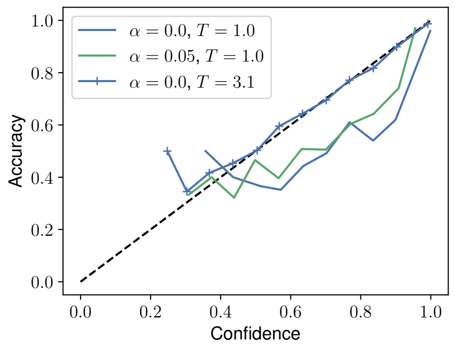

(b) ResNet-56 on the CIFAR-10 dataset

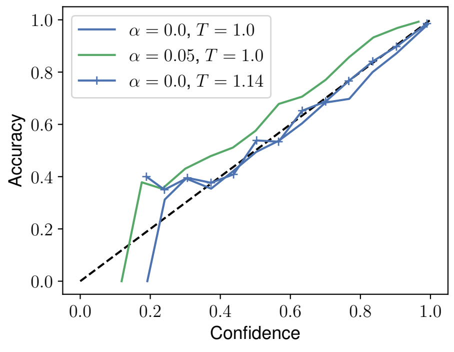

(c) FCN on the EMNIST dataset

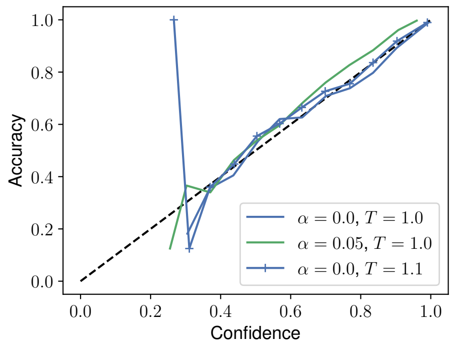

(d) FCN on the FMNIST dataset

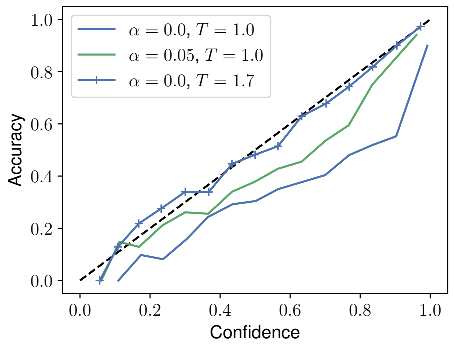

(e) ResNet-50 on the Tiny ImageNet dataset

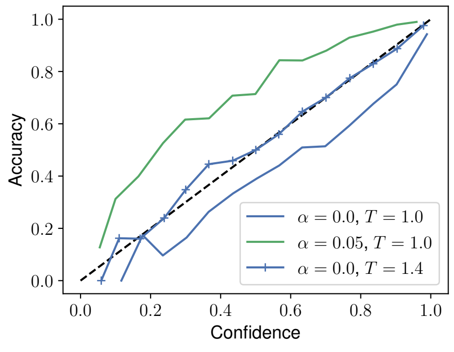

(f) ResNet-34 on the CUB-200-2011 dataset

Figure 9. Reliability diagrams for various classification networks.